

SUPPLEMENTARY MATERIALS

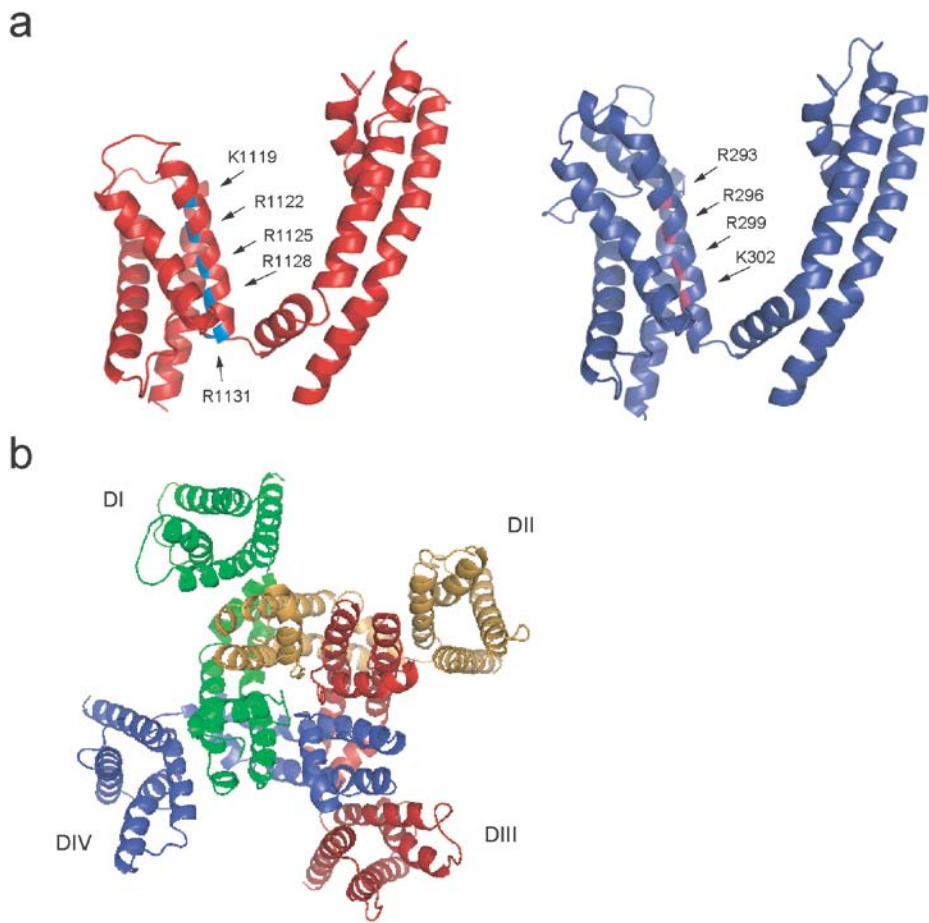
Molecular determinants of coupling between the DIII voltage-sensor and the pore of a sodium channel

Yukiko Muroi¹, Manoel Arcisio-Miranda¹, Sandipan Chowdhury and Baron Chanda

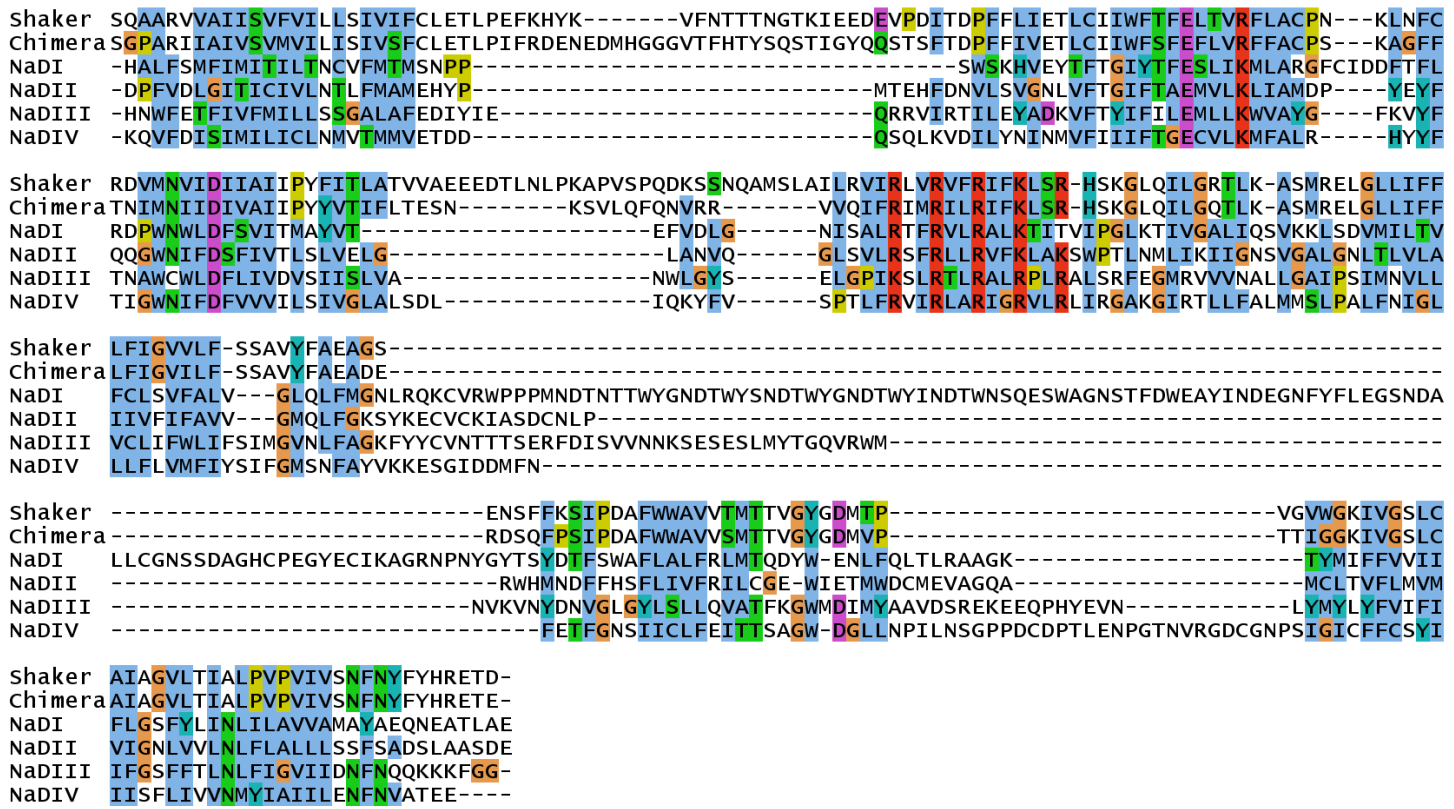
Department of Physiology, University of Wisconsin – Madison, 1300 University Ave., 129 SMI, Madison, Wisconsin 53706, USA.

¹ These authors contributed equally to this work

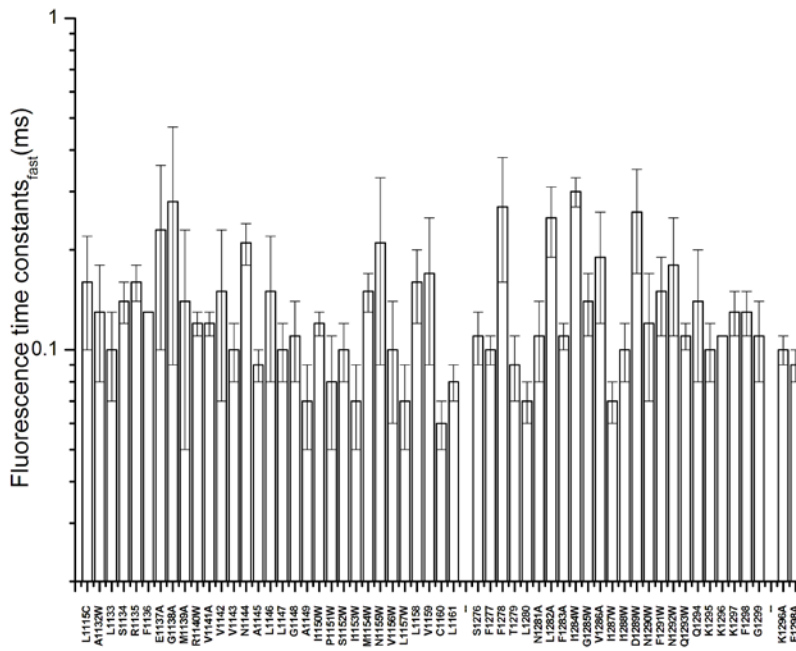
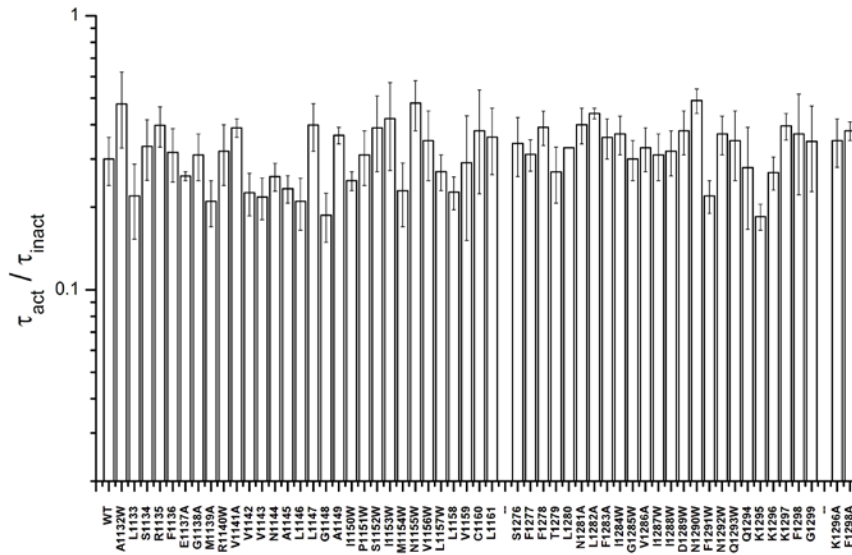
Correspondence should be addressed to B.C. (bchanda@physiology.wisc.edu)



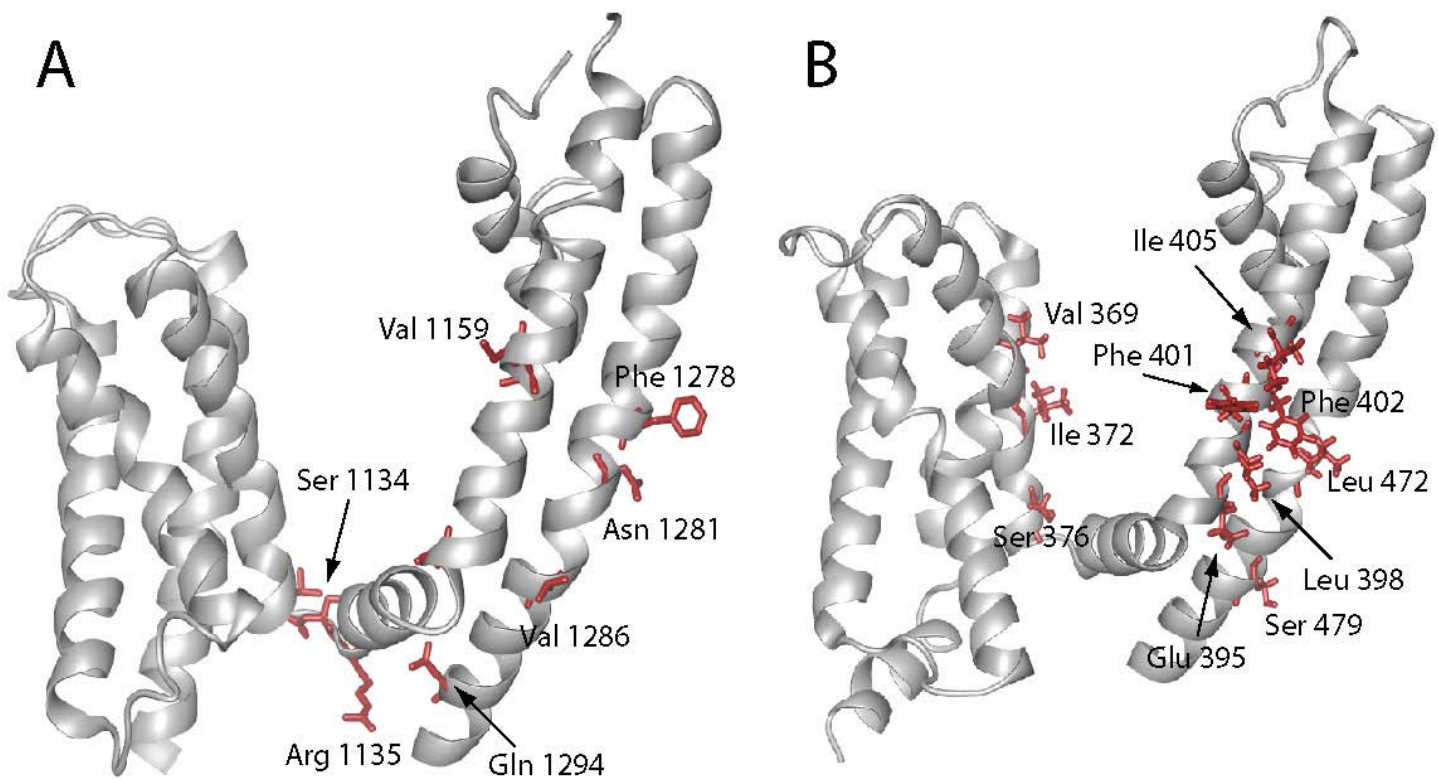
Supplementary figure 1: Structural model of rat skeletal muscle sodium channel generated from the Kv1.2/2.1 K channel chimera crystal structure. (a) Left: Homology model of Domain III of sodium channel. Charged residues in the S4 segment are highlighted in blue. Right: X-ray structure of a single subunit of K⁺ channel chimera (Kv1.2/2.1) (PDB code: 2R9R). (b) A top view of the homology model of sodium channel showing all the four domains. Green, orange, red, blue color represent domain I, II, III and IV of sodium channel, respectively.



Supplementary figure 2: A sequence alignment of the four domains (DI-DIV) of sodium channel with Kv1.2/2.1 chimera and Shaker potassium channels.



Supplementary Figure 3. A) The ratio of time constants of activation vs. inactivation obtained by fitting the inward sodium currents at potentials where the current reaches a maximum value. For the wild type sodium channels (L1115C mutant), the maximum current was observed at -15mV. The gating time constants for mutants E1137A, V1141A, L1158W, F1277W, Q1294W, F1298W, L1282A, V1286A, I1287W were obtained by fitting currents at -15 mV; G1138A, M1139A, M1154W, K1296W, V1156W and F1283A was obtained from currents at -20 mV; R1135W, S1134W, F1136W, V1143W, N1144W, A1145W, L1146W, G1148W, A1149W, T1279W, L1280W, K1297W and G1299W was obtained from currents at -10 mV; P1151W, I1284W and G1285W was obtained from currents at -25 mV; L1157W was obtained by fitting currents at -35 mV. B) The time constants of fast component of fluorescence from L1115C position for mutants and WT sodium channel. Previous studies have shown that the fast component of fluorescence from this position correlates with the activation time constants and the early component of gating (Chanda and Bezanilla, JGP (2002) 120:629-645). The plotted values were obtained from fluorescence signals recorded at +50 mV. Bars represent the mean value \pm S.E. of at least three independent experiments. Statistical analyses of ratios performed using one-way ANOVA with Dunnett's post-tests show that these ratios were not significantly different from the WT.



Supplementary Figure 4. Mapping the class II mutations onto the structural model of sodium channel domain III (A) and the Shaker potassium channel (B). The structure of the Shaker potassium channel was built using the Kv 1.2 structure (Long et. al. (2005) Science 309, 897-903) as a template. The class II mutations in the Shaker potassium channel were identified in previous studies (Smith-Maxwell et. al. (1998) J. Gen. Physiol. 111, 399-420; Smith-Maxwell et. al. (1998) J. Gen. Physiol. 111, 421-439; Ledwell and Aldrich (1999) J. Gen. Physiol. 113, 389-414, Soler-Llavina et. al. (2006) Neuron 52, 623-634).

Supplementary table I: Summary of F-V and G-V relationships of the WT and the mutants.

L1115C	F-V				G-V			
	n	V _{1/2} *	z	ΔV _{1/2}	n	V _{1/2}	z	ΔV _{1/2}
	11	-67.4 ± 2.7	1.42 ± 0.06		8	-26.3 ± 1.4	4.9 ± 0.7	
S4-S5 linker mutants								
A1132W	7	-66.0 ± 1.3	0.97 ± 0.09	1.4 ± 3.0	4	-9.1 ± 2.4	2.9 ± 0.1	17.2 ± 2.8
L1133W	4	-92.3 ± 5.2*	1.07 ± 0.08	-24.9 ± 5.8	4	-14.4 ± 1.7	3.4 ± 0.2	11.9 ± 2.2
S1134W	4	-94.4 ± 4.4*	1.14 ± 0.05	-27.0 ± 5.1	5	-21.1 ± 1.5	4.7 ± 0.8	5.2 ± 2.1
R1135W	6	-134.3 ± 1.0*	1.17 ± 0.03	-66.9 ± 2.9	4	-22.0 ± 2.1	3.2 ± 0.1	4.3 ± 2.5
F1136W	3	-72.9 ± 1.0	1.63 ± 0.03	-5.5 ± 2.9	6	-23.4 ± 3.0	4.2 ± 0.4	2.9 ± 3.3
E1137A	4	-64.8 ± 2.5	1.35 ± 0.12	2.6 ± 3.7	5	-28.3 ± 0.28	5.4 ± 0.4	-2.0 ± 1.4
G1138A	3	-80.9 ± 3.5*	1.15 ± 0.11	-13.6 ± 4.4	5	-28.2 ± 0.8	5.9 ± 0.7	-1.9 ± 1.6
M1139A	3	-99.5 ± 3.3*	0.93 ± 0.07	-32.1 ± 4.2	4	-28.3 ± 1.5	5.1 ± 0.5	-2.0 ± 2.1
R1140W	5	-71.5 ± 5.1	0.90 ± 0.06	-4.1 ± 5.7	4	-22.2 ± 1.3	5.0 ± 0.3	4.1 ± 1.9
V1141A	6	79.6 ± 1.7*	1.06 ± 0.07	-12.3 ± 3.2	5	-28.8 ± 1.6	5.6 ± 0.5	-2.5 ± 2.1
V1142W	3	-65.4 ± 5.4	1.44 ± 0.13	2.0 ± 6.0	4	-22.2 ± 1.0	3.3 ± 0.2	4.1 ± 1.7
V1143W	3	-79.9 ± 7.4	1.03 ± 0.03	-12.5 ± 7.9	5	-24.1 ± 2.3	4.3 ± 0.5	2.2 ± 2.7
N1144W	5	-41.0 ± 5.8*	1.55 ± 0.12	26.4 ± 6.4	7	-21.6 ± 2.2	5.4 ± 1.0	4.6 ± 2.6
A1145W	7	-75.3 ± 4.9	0.91 ± 0.07	-7.9 ± 5.5	7	-17.8 ± 2.9	4.2 ± 0.3	8.5 ± 3.2
L1146W	6	-80.7 ± 2.9*	1.29 ± 0.06	-13.4 ± 4.0	5	-26.3 ± 2.2	3.9 ± 0.4	-0.1 ± 2.6
L1147W	5	-70.4 ± 4.6	1.30 ± 0.10	-3.0 ± 5.3	7	-20.8 ± 10.9	4.6 ± 3.6	5.5 ± 11.0
G1148W	3	-66.6 ± 2.0	1.42 ± 0.08	0.8 ± 3.4	4	-24.6 ± 3.8	3.7 ± 0.9	1.7 ± 4.1
A1149W	6	-96.7 ± 4.1*	1.04 ± 0.05	-29.4 ± 4.9	5	-23.7 ± 2.3	3.8 ± 0.2	2.6 ± 2.7
I1150W	5	-88.2 ± 2.8*	0.95 ± 0.02	-20.8 ± 3.8	4	-26.6 ± 3.8	4.9 ± 0.8	-0.4 ± 4.0
P1151W	3	-79.2 ± 4.6*	1.36 ± 0.17	-11.8 ± 5.3	5	-37.9 ± 0.8	4.3 ± 0.3	-11.7 ± 1.6
S1152W	4	-62.0 ± 2.8	1.49 ± 0.14	5.3 ± 3.9	4	-23.1 ± 1.8	6.6 ± 0.6	3.2 ± 2.3
I1153W	5	-65.8 ± 2.1	1.14 ± 0.04	1.6 ± 3.4	4	-27.9 ± 1.3	6.5 ± 0.9	-1.6 ± 1.9
M1154W	4	-96.2 ± 4.7*	1.10 ± 0.08	-28.8 ± 5.4	4	-35.4 ± 2.0	5.5 ± 0.3	-9.2 ± 2.4
N1155W	3	-56.1 ± 3.5	1.75 ± 0.43	11.3 ± 4.4	4	-22.5 ± 0.9	5.5 ± 0.6	3.7 ± 1.6
V1156W	6	-88.6 ± 1.9*	0.99 ± 0.06	-21.2 ± 3.3	5	-34.6 ± 1.1	4.7 ± 0.1	-8.3 ± 1.8
L1157W	4	-89.3 ± 5.4*	0.99 ± 0.06	-22.0 ± 6.0	5	-44.6 ± 1.0	6.1 ± 0.3	-8.4 ± 1.7
L1158W	5	-72.0 ± 2.1	1.22 ± 0.10	-4.6 ± 3.4	5	-27.4 ± 0.8	4.6 ± 0.3	-1.1 ± 1.6
V1159W	3	-71.5 ± 1.5	1.25 ± 0.07	-4.1 ± 3.1	5	-16.2 ± 2.6	3.6 ± 0.2	10.0 ± 2.9
C1160W	5	-77.9 ± 2.6	1.25 ± 0.12	-10.5 ± 3.8	4	-21.8 ± 1.2	4.4 ± 0.2	4.5 ± 1.8
L1161W	3	-63.6 ± 1.8	1.37 ± 0.03	3.8 ± 3.2	4	-24.5 ± 0.9	5.7 ± 0.8	1.8 ± 1.6
S6 mutants								
S1276W	4	-74.3 ± 2.4	1.11 ± 0.11	-6.9 ± 3.6	5	-33.1 ± 3.2	5.1 ± 1.3	-6.8 ± 3.5
F1277W	6	-65.8 ± 2.6*	1.85 ± 0.23	1.6 ± 3.7	5	-31.1 ± 1.9	4.0 ± 0.2	-4.8 ± 2.3
F1278W	4	-78.3 ± 2.8	1.09 ± 0.11	-10.9 ± 3.8	4	-13.6 ± 1.5	4.5 ± 0.5	12.7 ± 2.0
T1279W	4	-73.2 ± 0.7	1.52 ± 0.07	-5.8 ± 2.8	4	-31.5 ± 4.6	3.4 ± 0.4	-5.2 ± 4.8
L1280W	3	-75.0 ± 2.2	1.37 ± 0.03	-7.6 ± 3.5	4	-23.3 ± 2.4	4.1 ± 0.2	3.0 ± 2.8
N1281A	5	-79.2 ± 1.6*	1.17 ± 0.11	-11.8 ± 3.1	4	-18.9 ± 0.9	5.1 ± 0.3	7.3 ± 1.6
L1282A	4	-91.2 ± 2.6*	1.25 ± 0.09	-23.8 ± 3.7	4	-31.0 ± 2.5	4.3 ± 0.3	-4.7 ± 2.9
F1283A	5	-86.3 ± 2.1*	1.12 ± 0.04	-19.0 ± 3.4	4	-34.1 ± 1.5	4.7 ± 0.7	-7.9 ± 2.1
I1284W	3	-83.2 ± 4.6*	1.56 ± 0.14	-15.8 ± 5.4	5	-37.2 ± 2.8	4.9 ± 0.4	-10.9 ± 3.1
G1285W	4	-72.1 ± 2.0	1.15 ± 0.03	-4.8 ± 3.3	5	-36.5 ± 1.9	5.0 ± 0.4	-10.2 ± 2.3

V1286A	5	-88.9 ± 1.4*	1.06 ± 0.05	-21.5 ± 3.0	5	-23.7 ± 0.9	5.4 ± 0.5	2.6 ± 1.6
I1287W	5	-78.9 ± 1.5*	1.28 ± 0.07	-11.5 ± 3.1	5	-33.9 ± 3.1	4.8 ± 0.3	-7.6 ± 3.3
I1288W	5	-59.5 ± 1.9	1.64 ± 0.27	7.9 ± 3.3	5	-21.1 ± 1.5	5.3 ± 0.7	5.2 ± 2.0
D1289A	4	-69.6 ± 1.3	1.05 ± 0.04	-2.2 ± 3.0	5	-22.4 ± 0.7	5.5 ± 0.2	3.9 ± 1.5
N1290W	4	-77.0 ± 2.1	1.10 ± 0.20	-9.6 ± 3.4	4	-22.3 ± 1.6	6.3 ± 0.3	3.9 ± 2.1
F1291W	5	-66.5 ± 3.3	1.07 ± 0.08	0.8 ± 4.2	5	-29.1 ± 1.4	4.4 ± 0.4	-2.8 ± 1.9
N1292W	6	-83.9 ± 3.6*	0.97 ± 0.09	-16.5 ± 4.5	5	-26.9 ± 1.0	6.0 ± 0.9	-0.6 ± 1.7
Q1293W	4	-69.6 ± 3.3	1.20 ± 0.07	-2.3 ± 4.3	4	-26.4 ± 0.7	4.8 ± 0.7	-0.1 ± 1.6
Q1294W	4	-50.4 ± 2.5*	1.58 ± 0.06	17.0 ± 3.7	4	-29.0 ± 3.5	4.3 ± 0.7	-2.7 ± 3.8
K1295W	4	-73.5 ± 3.8	1.24 ± 0.15	-6.1 ± 4.7	4	-31.0 ± 2.0	5.3 ± 0.7	-4.8 ± 2.4
K1296W	4	-64.1 ± 2.8	1.73 ± 0.18	3.3 ± 3.9	7	-34.8 ± 2.6	4.9 ± 0.7	-8.6 ± 2.9
K1297A	4	-55.2 ± 3.0*	1.42 ± 0.08	12.1 ± 4.0	5	-25.2 ± 0.7	7.7 ± 0.8	1.1 ± 1.5
F1298W	4	-60.4 ± 0.8	1.60 ± 0.10	7.0 ± 2.8	11	-28.3 ± 1.6	4.9 ± 0.2	-2.0 ± 2.1
G1299W	5	-57.4 ± 4.2	1.68 ± 0.20	10.0 ± 5.0	5	-25.8 ± 1.7	4.5 ± 0.3	0.5 ± 2.2
K1296A	4	-76.3 ± 2.0	1.01 ± 0.03	-8.9 ± 3.3	4	-27.8 ± 0.7	6.6 ± 0.3	-1.6 ± 1.5
F1298A	3	-82.2 ± 1.3	0.95 ± 0.02	-14.9 ± 3.0	4	-24.5 ± 0.8	7.6 ± 0.4	1.7 ± 1.6

Double mutant

R1135W-F1298R	3	-143.3 ± 0.7*	1.29 ± 0.01	-75.9 ± 2.8	4	-25.1 ± 1.0	6.5 ± 0.4	1.2 ± 1.6
---------------	---	---------------	-------------	-------------	---	-------------	-----------	-----------

Boltzmann parameters from a first-order fit of the F-V and G-V relationships. $V_{1/2}$ and z are mean ± S.E. of 3–11 independent experiments (n). $\Delta V_{1/2}$ is mean ± propagation of error. Statistical analysis of $V_{1/2}$ of F-V relationships was performed using a one-way ANOVA with Dunnett's post-tests, *p<0.05

Supplementary table II: Monotonicity of the probability expressions

Derivative	Expression	Monotonicity
Scheme IA		
$\frac{dP_{V_A}}{dK_1}$	$\frac{(1 + \theta K_2)(1 + K_2)}{(1 + K_1 + K_2 + \theta K_1 K_2)^2}$	>0
$\frac{dP_{P_O}}{dK_1}$	$\frac{K_2(\theta - 1)}{(1 + K_1 + K_2 + \theta K_1 K_2)^2}$	>0
$\frac{dP_{V_A}}{dK_2}$	$\frac{K_1(\theta - 1)}{(1 + K_1 + K_2 + \theta K_1 K_2)^2}$	>0
$\frac{dP_{P_O}}{dK_2}$	$\frac{(1 + \theta K_1)(1 + K_1)}{(1 + K_1 + K_2 + \theta K_1 K_2)^2}$	>0
$\frac{dP_{V_A}}{d\theta}$	$\frac{K_1 K_2 (1 + K_2)}{(1 + K_1 + K_2 + \theta K_1 K_2)^2}$	>0
$\frac{dP_{P_O}}{d\theta}$	$\frac{K_1 K_2 (1 + K_1)}{(1 + K_1 + K_2 + \theta K_1 K_2)^2}$	>0
Scheme IB		
$\frac{dP_{V_A}}{dK_1}$	$\frac{(1 + K_2)(\theta + K_2)}{(\theta + K_1 + K_2 + K_1 K_2)^2}$	>0
$\frac{dP_{P_O}}{dK_1}$	$\frac{K_2(\theta - 1)}{(\theta + K_1 + K_2 + K_1 K_2)^2}$	>0
$\frac{dP_{V_A}}{dK_2}$	$\frac{K_1(\theta - 1)}{(\theta + K_1 + K_2 + K_1 K_2)^2}$	>0
$\frac{dP_{P_O}}{dK_2}$	$\frac{(1 + K_1)(\theta + K_1)}{(\theta + K_1 + K_2 + K_1 K_2)^2}$	>0
$\frac{dP_{V_A}}{d\theta}$	$-\frac{(K_1 + K_1 K_2)}{(\theta + K_1 + K_2 + K_1 K_2)^2}$	<0
$\frac{dP_{P_O}}{d\theta}$	$-\frac{(K_2 + K_1 K_2)}{(\theta + K_1 + K_2 + K_1 K_2)^2}$	<0
Scheme II		
$\frac{dP_{V_A}}{dK_1}$	$\frac{(\theta + K_2)(1 + \theta K_2)}{(\theta + K_1 + K_2 + \theta K_1 K_2)^2}$	>0
$\frac{dP_{P_O}}{dK_1}$	$\frac{K_2(\theta^2 - 1)}{(\theta + K_1 + K_2 + \theta K_1 K_2)^2}$	>0
$\frac{dP_{V_A}}{dK_2}$	$\frac{K_1(\theta^2 - 1)}{(\theta + K_1 + K_2 + \theta K_1 K_2)^2}$	>0
$\frac{dP_{P_O}}{dK_2}$	$\frac{(\theta + K_1)(1 + \theta K_1)}{(\theta + K_1 + K_2 + \theta K_1 K_2)^2}$	>0
$\frac{dP_{V_A}}{d\theta}$	$\frac{K_1(K_2^2 - 1)}{(\theta + K_1 + K_2 + \theta K_1 K_2)^2}$	<0 ($K_2 < 1$)
$\frac{dP_{P_O}}{d\theta}$	$\frac{K_2(K_1^2 - 1)}{(\theta + K_1 + K_2 + \theta K_1 K_2)^2}$	>0 ($K_1 > 1$)

Scheme IA: Monotonicity of the probability expressions (from Scheme IA) with respect to the thermodynamic parameters. Monotonicity is expressed as > 0 (implying an increasing function of the parameter) or < 0 (implying a decreasing function of the parameter). **Scheme IB:** Monotonicity of the probability expressions (from Scheme IB) with respect to the thermodynamic parameters. Monotonicity is expressed as > 0 (implying an increasing function of the parameter) or < 0 (implying a decreasing function of the parameter). **Scheme II:** Monotonicity of the probability expressions (from Scheme II) with respect to the thermodynamic parameters. Monotonicity is expressed as > 0 (implying an increasing function of the parameter) or < 0 (implying a decreasing function of the parameter).